

Effects of Two-Phase Flow on the Deflagration of Porous Energetic Materials

Stephen B. Margolis*

Sandia National Laboratories, Livermore, California 94551-0969

and

Forman A. Williams†

University of California, San Diego, San Diego, California 92093-0310

Theoretical analyses are developed for the multiphase deflagration of porous energetic solids, such as degraded nitramine propellants, that experience significant gas flow in the solid preheat region and are characterized by the presence of exothermic reactions in a bubbling melt layer at their surfaces. Relative motion between the gas and condensed phases is taken into account in both regions, and expressions for the mass burning rate and other quantities of interest, such as temperature and volume-fraction profiles, are derived by activation-energy asymptotics. The model extends recent work by allowing for gas flow in the unburned solid, and by incorporating pressure effects through the gas-phase equation of state. As a consequence, it is demonstrated how most aspects of the deflagration wave, including its structure, propagation speed, and final temperature, depend on the local pressure in the two-phase regions.

I. Introduction

THE combustion behavior of energetic materials (e.g., solid propellants) has long been of interest in the fields of propulsion and pyrotechnics. In many such applications, it is becoming increasingly clear that two-phase flow effects play an important role, especially since during combustion, most homogeneous solid propellants develop thin multiphase layers at their surfaces in which finite rate exothermic reactions occur. In addition, there is a growing interest in the behavior of porous energetic solids, since even initially dense materials can develop significant void fractions if, at any time, they are exposed to sufficiently abnormal thermal environments. The deflagration characteristics of such “damaged” materials, with porosities as high as order unity, may then differ significantly from those of the pristine material due, at least in part, to greatly enhanced gas flow in the solid/gas preheat region. The presence of gas in the porous solid in turn results in a more pronounced two-phase effect in the multiphase surface layer, such as in the liquid melt region of nitramine propellants, which thus tend to exhibit extensive bubbling in an exothermic foam layer. The present analysis is largely applicable to this latter class of propellants.

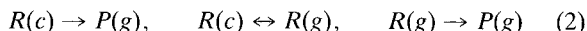
Describing phenomena associated with two-phase flow is inherently much more difficult than analyzing those occurring within a single phase. There are, first of all, certain fundamental difficulties that generally require the formulation of constitutive relations in order to obtain a closed model.^{1,2} Second, but of even greater significance from the standpoint of analysis, is the fact that the degree of nonlinearity in any model is increased by the appearance of appropriate volume-fraction variables that multiply each quantity associated with a particular phase. As a consequence, much of the early two-phase work in this area tended to treat the two-phase medium as a single phase with suitably “averaged” properties.^{3,4} This, in effect, requires the velocity (and temperature) of each phase

to be the same, precluding many of the predominant effects associated with combustion processes that involve two-phase flow.

We have recently addressed some of these concerns in several papers.^{5–7} To be able to focus clearly on the effects of two-phase flow, the description of the chemistry was deliberately simplified. In particular, a one-step exothermic process



was considered in Refs. 5 and 6, where $R(c)$ is the condensed (liquid) reactant, and $P(g)$ is the gaseous product. Thus, each phase is a pure species, and gas-phase reactions were either neglected or assumed to be remote, as was the solid/liquid interface. In Ref. 7, a more elaborate mechanism, motivated by knowledge of nitramine chemistry and given by



was adopted, where $R(g)$ is a gaseous reactant. In each of these studies, the goal was to clarify certain two-phase effects associated with different velocities (and in Refs. 5 and 6, temperatures) for each phase. Though not directly applicable to propellant deflagration, related two-phase modeling that accounts for velocity differences between phases has been used in the study of filtration combustion.^{8,9}

The purpose of the present work is to extend the analysis of Ref. 5 in several important respects. First, we formulate a more complete problem that explicitly includes melting of the unburned solid. Second, we assume that the unburned solid material has nonzero porosity, resulting in two-phase flow throughout the preheat and reaction zones. In our previous work, the effects of two-phase flow were confined to the reaction zone, which would be equivalent to assuming zero porosity for the solid in the present model. Finally, the fact that the gas phase exists throughout the unburned solid/liquid material leads us to relax the constant-density assumption that was adopted for the gas in our earlier work. In particular, we now allow for variable gas density according to a gas-phase equation of state that allows us to consider the effects of pressure on the various quantities of interest. These generalizations lead to a number of interesting effects directly at-

Received June 8, 1994; revision received Nov. 8, 1994; accepted for publication Dec. 2, 1994. This paper is declared a work of the U.S. Government and is not subject to copyright protection in the United States.

*Senior Member of Technical Staff, Combustion Research Facility.

†Professor, Department of Applied Mechanics and Engineering Sciences.

tributable to the influences of two-phase flow.¹⁰ For the present, we confine our attention to steady deflagration, leaving the consideration of instability and other nonsteady effects⁶ for future work.

To put what follows in better perspective, we note that there have been a number of early investigations specifically focused on the steady deflagration of porous energetic solids. The motivation for the work of Kuo and Summerfield,¹¹ e.g., was to explain the high deflagration velocities often observed for porous propellants. The physical explanation of the source of the increased burning velocity in this model was later clarified by Ermolayev et al.,¹² as arising from compressional heating rather than interphase convective heat transfer, and our allowance for variable gas density permits inclusion of effects of this type of heating. Earlier theoretical analyses of the combustion of porous propellants were published in the Russian literature and are cited in Refs. 11 and 12. Later formulations of equations for describing the combustion of porous materials were motivated, like the present work, also by the desire to be able to calculate unsteady processes as well. In that vein, Gough and Zwarts¹³ presented what, at that time, was the most logical set of conservation equations for combustion of porous propellants, excluding detonative transitions, and they clearly demonstrated inconsistencies in the equations employed in earlier works. Indeed, in a review of research performed prior to 1980, Gokhale and Krier¹⁴ acknowledge one such inconsistency in a footnote. More recent work by these and other authors has resulted in improved conservation equations, ultimately leading to the formulation of Baer and Nunziato,² which is one that has demonstrated the capability of calculating many time-dependent effects, including the transition from deflagration to detonation, and that can be considered to be the most general formulation currently available.

There are many possible pitfalls in attempting to formulate self-consistent conservation equations for multiphase combustion. For example, in some of the earlier work, there have been attempts to simplify the problem by ascribing the same hydrostatic pressure to the gaseous and condensed phases. However, in Eq. (10) of our previous paper⁵ we have shown that if there is interphase mass transfer between two phases and the average velocities of the two phases differ, then the average hydrostatic pressures in the two phases must also be allowed to differ for interface momentum conservation to be preserved. As the requisite modeling has evolved, such pitfalls have been recognized and avoided. For example, the approach in Ref. 13 properly takes into account the pressure difference between phases, as does the formulation of Baer and Nunziato.² For brevity in presenting the formulation employed here, we do not reiterate the full equations, but instead give only the simplified forms that will be needed in the subsequent analysis. Thus, e.g., the condensed-phase pressure will not appear in the following formulation, since compressibilities of condensed phases are negligible for the problems addressed here.

II. Formulation

A sketch of the physical problem is shown in Fig. 1. In an unconfined environment, the unburned porous solid lies generally to the left, and the burned gas products lie to the right. The two are separated by a deflagration wave that moves from right to left, converting the former into the latter. The structure of the combustion wave consists of a solid/gas preheat region, the melting surface that marks the left boundary of a liquid/gas preheat region, and a relatively thin exothermic reaction zone in which chemical reaction occurs according to Eq. (1). In what follows, we will restrict attention to one spatial dimension \bar{x} , and use the subscripts s , l , and g to denote solid, liquid, and gas-phase quantities, respectively. The porous solid thus extends to $\bar{x} = -\infty$, where conditions are denoted by the subscript u , while the product gases extend

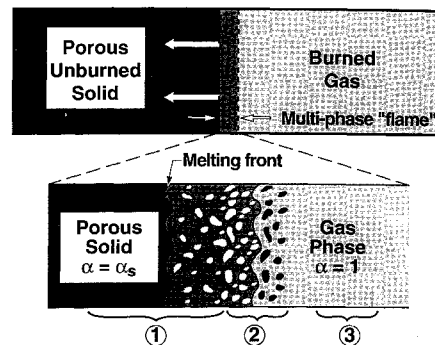


Fig. 1 Deflagration of a porous energetic material with two-phase flow in both the solid/gas and liquid/gas regions, with combustion occurring in the latter. The lower figure is a blowup of the multiphase "flame" structure, consisting minimally of ① a preheat zone containing a melting front across which the porous solid changes into a bubbly liquid, or foam and ② a thin liquid/gas reaction zone. Additional gas-phase reactions, suppressed in the present work, may occur in a secondary gas-flame region ③ downstream from the primary two-phase reaction zone ②.

to $\bar{x} = +\infty$, where conditions are identified by the subscript b . The appearance of a tilde over a symbol (e.g., $\tilde{\bar{x}}$) will denote a dimensional quantity.

The governing system of equations consists of conservation equations for continuity, momentum, and energy in the two-phase solid/gas and liquid/gas regions to the left and right of the melting surface $\bar{x} = \tilde{\bar{x}}_m$. Denoting the gas-phase volume fraction by α , continuity in the region $\bar{x} > \tilde{\bar{x}}_m$ is expressed separately for the liquid and gas phases as

$$\frac{\partial}{\partial t} [(1 - \alpha)\tilde{\rho}_l] + \frac{\partial}{\partial \bar{x}} [(1 - \alpha)\tilde{\rho}_l\tilde{u}_l] = -\tilde{A}\tilde{\rho}_l(1 - \alpha)\exp(-\tilde{E}_l/\tilde{R}^0\tilde{T}_l), \quad \bar{x} > \tilde{\bar{x}}_m \quad (3)$$

$$\frac{\partial}{\partial t} (\alpha\tilde{\rho}_g) + \frac{\partial}{\partial \bar{x}} (\alpha\tilde{\rho}_g\tilde{u}_g) = \tilde{A}\tilde{\rho}_l(1 - \alpha)\exp(-\tilde{E}_l/\tilde{R}^0\tilde{T}_l), \quad \bar{x} > \tilde{\bar{x}}_m \quad (4)$$

where $\tilde{\rho}$, \tilde{u} , \tilde{T} , and \tilde{t} denote density, velocity, temperature, and time, respectively. For simplicity, we will assume a constant value for $\tilde{\rho}_l$, but not for $\tilde{\rho}_g$. As discussed in Ref. 5, the evaluation of the Arrhenius reaction rate is based on conditions (e.g., temperature) in the liquid phase, and may be interpreted as a contribution to a constitutive relation for that medium. In that expression, \tilde{E}_l is the overall activation energy, \tilde{R}^0 is the universal gas constant, and \tilde{A} is the exponential reciprocal-time prefactor which, for simplicity, will be assumed constant. For this type of global kinetic modeling, however, it may be reasonable to assign a pressure, as well as a temperature dependency to \tilde{A} . Finally, in place of Eq. (4), it is convenient to use the overall liquid/gas continuity equation, obtained by summing Eqs. (3) and (4) as

$$\frac{\partial}{\partial t} [(1 - \alpha)\tilde{\rho}_l + \alpha\tilde{\rho}_g] + \frac{\partial}{\partial \bar{x}} [(1 - \alpha)\tilde{\rho}_l\tilde{u}_l + \alpha\tilde{\rho}_g\tilde{u}_g] = 0 \quad \bar{x} > \tilde{\bar{x}}_m \quad (5)$$

In the solid/gas region $\bar{x} < \tilde{\bar{x}}_m$, we assume for the solid phase a constant density $\tilde{\rho}_s$ and zero velocity ($\tilde{u}_s = 0$), with $\alpha = \alpha_s$ also constant in this region. Gas-phase continuity for $\bar{x} < \tilde{\bar{x}}_m$ is thus independent of the solid phase and is given by

$$\frac{\partial \tilde{\rho}_g}{\partial t} + \frac{\partial}{\partial \bar{x}} (\tilde{\rho}_g\tilde{u}_g) = 0, \quad \bar{x} < \tilde{\bar{x}}_m \quad (6)$$

Conservation of energy for each phase in the liquid/gas region is given by

$$\begin{aligned} \frac{\partial}{\partial t} [\bar{\rho}_l \bar{c}_l (1 - \alpha) \bar{T}_l] + \frac{\partial}{\partial \bar{x}} [\bar{\rho}_l \bar{c}_l \bar{u}_l (1 - \alpha) \bar{T}_l] \\ - \frac{\partial}{\partial \bar{x}} \left[\bar{\lambda}_l (1 - \alpha) \frac{\partial \bar{T}_l}{\partial \bar{x}} \right] = \bar{Q} \bar{A} \bar{\rho}_l (1 - \alpha) \exp(-\bar{E}_l / \bar{R}^0 \bar{T}_l) \\ + \bar{K}_{lg} (\bar{T}_g - \bar{T}_l), \quad \bar{x} > \bar{x}_m \end{aligned} \quad (7)$$

$$\begin{aligned} \frac{\partial}{\partial t} (\bar{\rho}_g \bar{c}_g \alpha \bar{T}_g) + \frac{\partial}{\partial \bar{x}} (\bar{\rho}_g \bar{c}_g \bar{u}_g \alpha \bar{T}_g) - \frac{\partial}{\partial \bar{x}} \left(\bar{\lambda}_g \alpha \frac{\partial \bar{T}_g}{\partial \bar{x}} \right) \\ = \alpha \frac{\partial \bar{p}_g}{\partial t} + \bar{K}_{lg} (\bar{T}_l - \bar{T}_g), \quad \bar{x} > \bar{x}_m \end{aligned} \quad (8)$$

where \bar{c} , $\bar{\lambda}$, and \bar{p} denote heat capacity (at constant volume for the liquid, and at constant pressure for the gas, both assumed constant), thermal conductivity and pressure, respectively, \bar{Q} is the heat release for the global reaction (1) at temperature \bar{T}_l , and \bar{K}_{lg} is an interphase heat-transfer coefficient.⁵ Because of the small Mach number and the small ratio of gas-to-liquid densities in the problems to be considered, no terms involving the liquid pressure \bar{p}_l appear in Eq. (7), and the gas pressure \bar{p}_g depends only on \bar{t} in Eq. (8). We remark that the term involving \bar{p}_g arises from the contribution to the rate of change of the internal energy of the gas from the sum of the rate of surface work $-\partial(\alpha \bar{u}_g \bar{p}_g)/\partial \bar{x}$ and the rate of volume work $-\bar{p}_g \partial \alpha / \partial t$ performed by the gas. Relating the internal energy \bar{e}_g of the gas to its enthalpy \bar{h}_g according to the thermodynamic identity $\bar{e}_g = \bar{h}_g - \bar{p}_g / \bar{\rho}_g$ then results in the first term on the right-hand side (RHS) of Eq. (8).

As in the case of overall continuity, we will use in place of Eq. (8) the overall liquid/gas energy equation [the sum of Eqs. (7) and (8)], and, in addition, use liquid-phase continuity, Eq. (3), to eliminate the reaction-rate terms in this equation and in Eq. (7). Thus, in place of Eqs. (7) and (8), we have the liquid and overall energy equations

$$\begin{aligned} \frac{\partial}{\partial t} [\bar{\rho}_l (1 - \alpha) (\bar{Q} + \bar{c}_l \bar{T}_l)] + \frac{\partial}{\partial \bar{x}} [\bar{\rho}_l \bar{u}_l (1 - \alpha) (\bar{Q} + \bar{c}_l \bar{T}_l)] \\ - \frac{\partial}{\partial \bar{x}} \left[\bar{\lambda}_l (1 - \alpha) \frac{\partial \bar{T}_l}{\partial \bar{x}} \right] = \bar{K}_{lg} (\bar{T}_g - \bar{T}_l), \quad \bar{x} > \bar{x}_m \end{aligned} \quad (9)$$

$$\begin{aligned} \frac{\partial}{\partial t} [\bar{\rho}_l (1 - \alpha) (\bar{Q} + \bar{c}_l \bar{T}_l) + \bar{\rho}_g \bar{c}_g \alpha \bar{T}_g] \\ + \frac{\partial}{\partial \bar{x}} [\bar{\rho}_l \bar{u}_l (1 - \alpha) (\bar{Q} + \bar{c}_l \bar{T}_l) + \bar{\rho}_g \bar{c}_g \bar{u}_g \alpha \bar{T}_g] \\ = \frac{\partial}{\partial \bar{x}} \left[\bar{\lambda}_l (1 - \alpha) \frac{\partial \bar{T}_l}{\partial \bar{x}} + \bar{\lambda}_g \alpha \frac{\partial \bar{T}_g}{\partial \bar{x}} \right] + \alpha \frac{\partial \bar{p}_g}{\partial t}, \quad \bar{x} > \bar{x}_m \end{aligned} \quad (10)$$

In a similar fashion, conservation of energy in the solid/gas region is expressed as

$$\begin{aligned} \frac{\partial}{\partial t} [\bar{\rho}_s \bar{c}_s (1 - \alpha_s) \bar{T}_s] - \frac{\partial}{\partial \bar{x}} \left[\bar{\lambda}_s (1 - \alpha_s) \frac{\partial \bar{T}_s}{\partial \bar{x}} \right] \\ = \bar{K}_{sg} (\bar{T}_g - \bar{T}_s), \quad \bar{x} < \bar{x}_m \end{aligned} \quad (11)$$

$$\begin{aligned} \frac{\partial}{\partial t} [\bar{\rho}_s \bar{c}_s (1 - \alpha_s) \bar{T}_s + \bar{\rho}_g \bar{c}_g \alpha_s \bar{T}_g] + \frac{\partial}{\partial \bar{x}} (\bar{\rho}_g \bar{c}_g \bar{u}_g \alpha_s \bar{T}_g) \\ = \frac{\partial}{\partial \bar{x}} \left[\bar{\lambda}_s (1 - \alpha_s) \frac{\partial \bar{T}_s}{\partial \bar{x}} + \bar{\lambda}_g \alpha_s \frac{\partial \bar{T}_g}{\partial \bar{x}} \right] + \alpha_s \frac{\partial \bar{p}_g}{\partial t}, \quad \bar{x} < \bar{x}_m \end{aligned} \quad (12)$$

where Eq. (12) describes overall energy conservation and is obtained by summing Eq. (11) for the solid and the corresponding equation for the gas phase.

Although analogous equations may be written for momentum conservation, they do not need to be introduced explicitly for the present class of problems. As remarked above, the approximation of small Mach number implies that the gas pressure \bar{p}_g is independent of the spatial coordinate. The gas is assumed to be ideal, where \bar{p}_g is coupled to the other field variables through the gas-phase equation of state

$$\bar{p}_g = \bar{\rho}_g \bar{R}^0 \bar{T}_g / \bar{W}_g \quad (13)$$

where \bar{W}_g is the molecular weight of the product gas. Consideration of condensed-phase momentum leads, in principle, to an equation for the liquid-phase velocity \bar{u}_l .⁵ This, however, introduces considerable additional complexity into the problem and involves introducing momentum-transfer parameters and other quantities that are difficult to determine. Accordingly, early studies^{3,4} tended to invoke the simple assumption that condensed- and gas-phase velocities were identical; i.e., $\bar{u}_l = \bar{u}_g$. More recent work, however, has shown that such an approximation not only violates order-of-magnitude estimates made in momentum conservation,⁵ but also fails to account for potentially significant phenomena associated with convective enthalpy transport by the gas relative to enthalpy transport in the condensed phases.¹⁰ On the other hand, the approximation that the condensed velocity equal the condensed mass burning rate divided by the condensed-phase density is consistent with momentum conservation in the absence of viscous and surface-tension-gradient forces.⁵ In the present context, this implies that, since $\bar{u}_s = 0$

$$\bar{u}_l = - \frac{d\bar{x}_m}{dt} \left(\frac{\bar{\rho}_s}{\bar{\rho}_l} - 1 \right) \quad (14)$$

where $d\bar{x}_m/dt < 0$ is the (unknown) propagation velocity of the melting surface. When these forces are present, viscosity tends to increase \bar{u}_l (since $\bar{u}_g > \bar{u}_l$), whereas surface-tension gradients tend to decrease \bar{u}_l . Order-of-magnitude estimates suggest that the former effect is negligible, while the latter may be more pronounced,⁵ leading to a decreasing evolutionary dependence of \bar{u}_l with respect to the volume fraction α . Postulating this dependence to be linear, Eq. (14) may be generalized according to

$$\bar{u}_l = - \frac{d\bar{x}_m}{dt} \left[\frac{\bar{\rho}_s}{\bar{\rho}_l} (1 - s\alpha) - 1 \right] \quad (15)$$

where an expression for the parameter $s > 0$, representing the difference between Marangoni and viscous effects, was derived previously.⁵ For simplicity, and because of uncertainties in values of surface tensions, we will mainly confine our attention in the present work to the case $s = 0$, although certain results for $s \neq 0$ will also be given.

The above equations now constitute a closed set for the variables α , \bar{u}_g , \bar{T}_l , \bar{T}_g , $\bar{\rho}_g$, and \bar{p}_g . The problem is thus completely determined once initial and boundary conditions (including interface relations at $\bar{x} = \bar{x}_m$) are specified. In the present work, we will not be concerned with the initial-value problem, but only the long-time solution corresponding to a steadily propagating deflagration. Thus, the required boundary conditions are given by

$$\alpha = \alpha_s \quad \text{for} \quad \bar{x} < \bar{x}_m \quad (16)$$

$$\bar{u}_g \rightarrow 0, \quad \bar{T}_g \rightarrow \bar{T}_s \rightarrow \bar{T}_u \quad \text{as} \quad \bar{x} \rightarrow -\infty$$

$$\alpha \rightarrow 1, \quad \bar{p}_g \rightarrow \bar{p}_g^0, \quad \bar{T}_l \rightarrow \bar{T}_g \rightarrow \bar{T}_b \quad \text{as} \quad \bar{x} \rightarrow +\infty \quad (17)$$

where the burned temperature \bar{T}_b is to be determined, and the boundary condition on pressure implies that $\bar{p}_g = \bar{p}_g^0$ every-

where. Finally, denoting by \pm superscripts quantities evaluated at $\bar{x} = \bar{x}_m^\pm$, the continuity and jump conditions across the melting surface are

$$\bar{\rho}_g^- = \bar{\rho}_g^+ \quad (18)$$

$$\bar{T}_g^- = \bar{T}_g^+, \quad \bar{T}_s^- = \bar{T}_s^+ \equiv \bar{T}_m \quad (19)$$

conservation of condensed- and gas-phase mass fluxes

$$(1 - \alpha_s)\bar{\rho}_s \left(-\frac{d\bar{x}_m}{dt} \right) = (1 - \alpha^+)\bar{\rho}_l \left(\bar{u}_l^+ - \frac{d\bar{x}_m}{dt} \right) \quad (20)$$

$$\alpha_s \left(\bar{u}_g^- - \frac{d\bar{x}_m}{dt} \right) = \alpha^+ \left(\bar{u}_g^+ - \frac{d\bar{x}_m}{dt} \right) \quad (21)$$

and conservation of condensed- and gas-phase enthalpy fluxes

$$\begin{aligned} (1 - \alpha^+)\bar{\lambda}_l \frac{d\bar{T}_l}{d\bar{x}} \Big|_{\bar{x}=\bar{x}_m^+} - (1 - \alpha_s)\bar{\lambda}_s \frac{d\bar{T}_s}{d\bar{x}} \Big|_{\bar{x}=\bar{x}_m^-} \\ = \bar{\rho}_s \bar{\gamma}_s (1 - \alpha_s) \frac{d\bar{x}_m}{dt} + \left[\bar{\rho}_l \bar{c}_l (1 - \alpha^+) \left(\bar{u}_l^+ - \frac{d\bar{x}_m}{dt} \right) \right. \\ \left. - \bar{\rho}_s \bar{c}_s (1 - \alpha_s) \left(-\frac{d\bar{x}_m}{dt} \right) \right] \bar{T}_m \end{aligned} \quad (22)$$

$$\alpha^+ \bar{\lambda}_g \frac{d\bar{T}_g}{d\bar{x}} \Big|_{\bar{x}=\bar{x}_m^+} - \alpha_s \bar{\lambda}_g \frac{d\bar{T}_g}{d\bar{x}} \Big|_{\bar{x}=\bar{x}_m^-} = 0 \quad (23)$$

where $\bar{\gamma}_s$ is the heat of melting of the solid at temperature $\bar{T} = 0$ ($\bar{\gamma}_s$ being negative when melting is endothermic). From Eqs. (15), (20), and (21) we obtain the relations:

$$\alpha^+ \bar{u}_g^+ - \alpha_s \bar{u}_g^- = -\frac{d\bar{x}_m}{dt} (\alpha_s - \alpha^+) \quad (24)$$

$$\alpha_s - \alpha^+ = s\alpha^+(1 - \alpha^+) \quad (25)$$

In the limit $s = 0$, Eqs. (24) and (25) reduce to the statement that α and \bar{u}_g are continuous across $\bar{x} = \bar{x}_m$.

III. Nondimensionalizations and the Steady-State Problem

In the present work, we will confine our attention to the case of a steadily propagating deflagration that propagates with the (unknown) speed $\bar{U} = -d\bar{x}_m/dt$, which is a convenient characteristic velocity for the problem. Assuming constant values for heat capacities and thermal conductivities, we then introduce the nondimensional variables

$$\begin{aligned} x = \frac{\bar{\rho}_s \bar{c}_s \bar{U}}{\bar{\lambda}_s} \bar{x}, \quad t = \frac{\bar{\rho}_s \bar{c}_s \bar{U}^2}{\bar{\lambda}_s} \bar{t}, \quad T_{s,l,g} = \frac{\bar{T}_{s,l,g}}{\bar{T}_u} \\ u_{l,g} = \frac{\bar{u}_{l,g}}{\bar{U}}, \quad \rho_g = \frac{\bar{\rho}_g}{\bar{\rho}_g^u} \end{aligned} \quad (26)$$

where $\bar{\rho}_g^u = \bar{\rho}_g^0 \bar{W}_g / \bar{R}^0 \bar{T}_u$ denotes the gas density at the unburned temperature \bar{T}_u . In addition, the nondimensional parameters

$$\begin{aligned} r = \frac{\bar{\rho}_l}{\bar{\rho}_s}, \quad \hat{r} = \frac{\bar{\rho}_g^u}{\bar{\rho}_s}, \quad l = \frac{\bar{\lambda}_l}{\bar{\lambda}_s}, \quad \hat{l} = \frac{\bar{\lambda}_g}{\bar{\lambda}_s}, \quad b = \frac{\bar{c}_l}{\bar{c}_s} \\ \hat{b} = \frac{\bar{c}_g}{\bar{c}_s}, \quad \gamma_s = \frac{\bar{\gamma}_s}{\bar{c}_s \bar{T}_u}, \quad Q = \frac{\bar{Q}}{\bar{c}_s \bar{T}_u}, \quad K_{sg} = \frac{\bar{\lambda}_s \bar{K}_{sg}}{\bar{\rho}_s^2 \bar{c}_s^2 \bar{U}^2} \\ K_{lg} = \frac{\bar{\lambda}_s \bar{K}_{lg}}{r b \bar{\rho}_s^2 \bar{c}_s^2 \bar{U}^2}, \quad N = \frac{\bar{E}_l}{\bar{R}^0 \bar{T}_b}, \quad \Lambda = \frac{\bar{\lambda}_s \bar{A}}{\bar{\rho}_s \bar{c}_s \bar{U}^2} e^{-N} \end{aligned} \quad (27)$$

are defined. It may be remarked that Λ is the appropriate burning-rate eigenvalue, the determination of which will provide the propagation speed \bar{U} .

Transforming to the moving coordinate $\xi = x + t$, whose origin is defined to be x_m , and introducing the above nondimensionalizations, steadily propagating deflagrations for the problem formulated in Sec. II will be determined as solutions of the steady eigenvalue problem

$$\frac{d}{d\xi} [\rho_g(u_g + 1)] = 0, \quad \xi < 0 \quad (28)$$

$$\frac{d}{d\xi} [r(1 - \alpha)(u_l + 1) + \hat{r}\alpha\rho_g(u_g + 1)] = 0, \quad \xi > 0 \quad (29)$$

$$\frac{d}{d\xi} [(1 - \alpha)(u_l + 1)] = -\Lambda(1 - \alpha)\exp \left[N \left(1 - \frac{T_b}{T_l} \right) \right] \quad \xi > 0 \quad (30)$$

$$(1 - \alpha_s) \left(\frac{dT_s}{d\xi} - \frac{d^2 T_s}{d\xi^2} \right) = K_{sg}(T_g - T_s), \quad \xi < 0 \quad (31)$$

$$\begin{aligned} r \frac{d}{d\xi} [(1 - \alpha)(u_l + 1)(Q + bT_l)] = l \frac{d}{d\xi} \left[(1 - \alpha) \frac{dT_l}{d\xi} \right] \\ + r b K_{lg}(T_g - T_l), \quad \xi > 0 \end{aligned} \quad (32)$$

$$\begin{aligned} (1 - \alpha_s) \frac{dT_s}{d\xi} + \hat{r} b \alpha_s \frac{d}{d\xi} (u_g + 1) \\ = \frac{d}{d\xi} \left[(1 - \alpha_s) \frac{dT_s}{d\xi} + \hat{l} \alpha_s \frac{dT_g}{d\xi} \right], \quad \xi < 0 \end{aligned} \quad (33)$$

$$\begin{aligned} \frac{d}{d\xi} [r(1 - \alpha)(u_l + 1)(Q + bT_l) + \hat{r} b \alpha(u_g + 1)\rho_g T_g] \\ = \frac{d}{d\xi} \left[l(1 - \alpha) \frac{dT_l}{d\xi} + \hat{l} \alpha \frac{dT_g}{d\xi} \right], \quad \xi > 0 \end{aligned} \quad (34)$$

$$\rho_g T_g = 1 \quad (35)$$

$$u_l = (1/r)(1 - r - s\alpha) \quad (36)$$

subject to the boundary conditions

$$\alpha = \alpha_s \quad \text{for } \xi < 0 \quad (37)$$

$$u_g \rightarrow 0, \quad T_g \rightarrow T_s \rightarrow 1 \quad \text{as } \xi \rightarrow -\infty$$

$$\alpha \rightarrow 1, \quad T_l \rightarrow T_g \rightarrow T_b \quad \text{as } \xi \rightarrow +\infty \quad (38)$$

and the melting-surface ($\xi = 0$) conditions

$$T_s^- = T_l^+ = T_m, \quad T_g^- = T_g^+ \quad (39)$$

$$\alpha^+(u_g^+ + 1) = \alpha_s(u_g^- + 1), \quad \alpha_s - \alpha^+ = s\alpha^+(1 - \alpha^+) \quad (40)$$

$$\alpha^+ \frac{dT_g}{d\xi} \Big|_{\xi=0^+} - \alpha_s \frac{dT_g}{d\xi} \Big|_{\xi=0^-} = 0 \quad (41)$$

$$\begin{aligned} l(1 - \alpha^+) \frac{dT_l}{d\xi} \Big|_{\xi=0^+} - (1 - \alpha_s) \frac{dT_s}{d\xi} \Big|_{\xi=0^-} = -(1 - \alpha_s)\gamma_s \\ + [b(1 - \alpha^+)(1 - s\alpha^+) - (1 - \alpha_s)]T_m \end{aligned} \quad (42)$$

We remark that Eqs. (28–30) were obtained directly from the continuity Eqs. (3), (5), and (6), and Eqs. (31–34) were obtained from Eqs. (9–12) using the gas-phase equation of state (13).

Thus, the final model for steady, planar deflagration that has been derived is given by Eqs. (28–42). An important and realistic limiting case, which results in some additional simplification, is to consider the limit of infinitely fast interphase heat transfer (i.e., $K_{sg}, K_{lg} \rightarrow \infty$). In that limit, Eqs. (31) and (32) imply that $T_s = T_g \equiv T$ in the region $\xi < 0$, and $T_l = T_g \equiv T$ in the region $\xi > 0$. The model then reduces to a single-temperature model, which is analyzed in the next section. The case of large, but finite, values of the interphase heat-transfer coefficients, which permit separate temperatures for each phase, is then considered in a subsequent section. Both cases will be analyzed in the limit of large activation energy ($N \gg 1$).

IV. Analysis of the Single-Temperature Model

In the limit that K_{sg} and K_{lg} are both infinite, the model (28–42) reduces, in the limit $s = 0$, to a subproblem written in terms of the single temperature variable T that denotes the common temperature of all phases at a given spatial location. In particular, we obtain in this limit the reduced problem given by

$$\frac{d}{d\xi} \left[\frac{1}{T} (u_g + 1) \right] = 0, \quad \xi < 0 \quad (43)$$

$$\frac{d}{d\xi} \left[(1 - \alpha) + \hat{r}\alpha \frac{1}{T} (u_g + 1) \right] = 0, \quad \xi > 0 \quad (44)$$

$$\frac{d}{d\xi} (1 - \alpha) = -r\Lambda(1 - \alpha) \exp \left[N \left(1 - \frac{T_b}{T} \right) \right], \quad \xi > 0 \quad (45)$$

$$\begin{aligned} (1 - \alpha_s) \frac{dT}{d\xi} + \hat{r}\hat{b}\alpha_s \frac{d}{d\xi} (u_g + 1) \\ = \frac{d}{d\xi} \left[(1 - \alpha_s + \hat{l}\alpha_s) \frac{dT}{d\xi} \right], \quad \xi < 0 \end{aligned} \quad (46)$$

$$\begin{aligned} \frac{d}{d\xi} [(1 - \alpha)(Q + bT) + \hat{r}\hat{b}\alpha(u_g + 1)] \\ = \frac{d}{d\xi} \left\{ [l(1 - \alpha) + \hat{l}\alpha] \frac{dT}{d\xi} \right\}, \quad \xi > 0 \end{aligned} \quad (47)$$

subject to

$$u_g \rightarrow 0, \quad T \rightarrow 1 \quad \text{as} \quad \xi \rightarrow -\infty \quad (48)$$

$$\alpha \rightarrow 1, \quad T \rightarrow T_b \quad \text{as} \quad \xi \rightarrow +\infty \quad (49)$$

$$T = T_m, \quad \alpha = \alpha_s, \quad u_g \text{ continuous at } \xi = 0 \quad (50)$$

$$\begin{aligned} [l(1 - \alpha_s) + \hat{l}\alpha_s] \frac{dT}{d\xi} \Big|_{\xi=0^+} - (1 - \alpha_s + \hat{l}\alpha_s) \frac{dT}{d\xi} \Big|_{\xi=0^-} \\ = (1 - \alpha_s)[- \gamma_s + (b - 1)T_m] \end{aligned} \quad (51)$$

where the overall enthalpy-flux conservation condition (51) is obtained from the sum of Eqs. (41) and (42), and where the final burned temperature T_b and the flame-speed eigenvalue Λ are to be determined.

The solution in the region $\xi < 0$, where chemical activity is absent, as well as expressions for T_b and $u_{g,\infty} \equiv u_g|_{\xi=\infty}$, are obtained as follows. From Eqs. (43) and (48), we have

$$u_g + 1 = T, \quad \xi < 0 \quad (52)$$

and hence, $u_g|_{\xi=0} = T_m - 1$. Equations (44) and (50) then imply

$$u_g + 1 = \frac{\alpha + \alpha_s(\hat{r} - 1)}{\alpha\hat{r}} T, \quad \xi > 0 \quad (53)$$

which, upon evaluation at $\xi = \infty$, determines $u_{g,\infty}$ in terms of T_b through Eq. (49) as

$$u_{g,\infty} = \frac{1 + \alpha_s(\hat{r} - 1)}{\hat{r}} T_b - 1 \quad (54)$$

Turning attention to the energy Eqs. (46) and (47), we may readily perform a single integration and use Eqs. (52–54) to obtain

$$[1 + \alpha_s(\hat{r}\hat{b} - 1)](T - 1) = (1 - \alpha_s + \hat{l}\alpha_s) \frac{dT}{d\xi}, \quad \xi < 0 \quad (55)$$

$$\begin{aligned} \{b(1 - \alpha) + \hat{b}[\alpha + \alpha_s(\hat{r} - 1)]\}T = [l(1 - \alpha) + \hat{l}\alpha] \frac{dT}{d\xi} \\ - (1 - \alpha)Q + \hat{b}[1 + \alpha_s(\hat{r} - 1)]T_b, \quad \xi > 0 \end{aligned} \quad (56)$$

A second integration of Eq. (55) then implies that

$$T(\xi) = 1 + (T_m - 1) \exp \left[\frac{1 + \alpha_s(\hat{r}\hat{b} - 1)}{1 + \alpha_s(\hat{l} - 1)} \xi \right], \quad \xi < 0 \quad (57)$$

which, from Eq. (52), also determines $u_g(\xi)$ in the region $\xi < 0$. In addition, subtracting Eq. (55) evaluated at $\xi = 0^-$ from Eq. (56) evaluated at $\xi = 0^+$ and using the jump condition (51), we obtain a relation for T_b given by

$$T_b = \frac{(1 - \alpha_s)(Q + 1 + \gamma_s) + \hat{r}\hat{b}\alpha_s}{\hat{b}[1 + \alpha_s(\hat{r} - 1)]} \quad (58)$$

which, from Eq. (54), determines $u_{g,\infty}$ as

$$u_{g,\infty} = (\hat{r}\hat{b})^{-1}(1 - \alpha_s)(Q + 1 + \gamma_s - \hat{r}\hat{b}) \quad (59)$$

It can be shown by means of similar manipulations that identical results (58) and (59) are obtained from the two-temper-

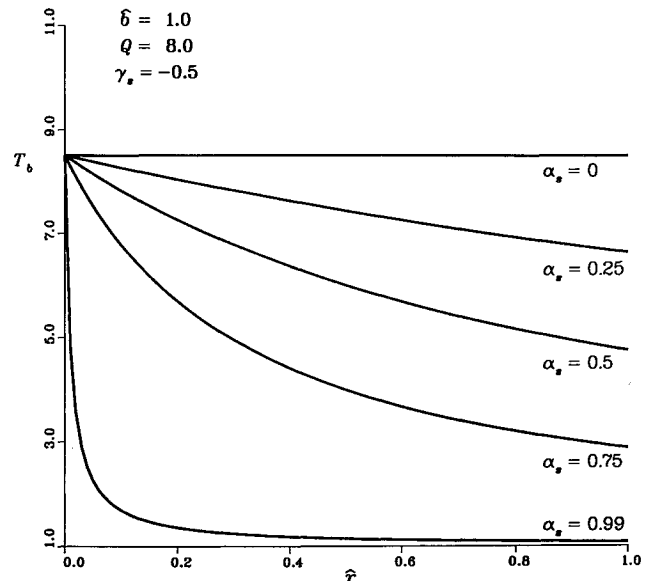


Fig. 2 Final burned temperature T_b as a function of the gas-to-solid density ratio \hat{r} , where the latter is proportional to the gas-phase pressure, for several values of the initial gas-phase volume fraction α_s .

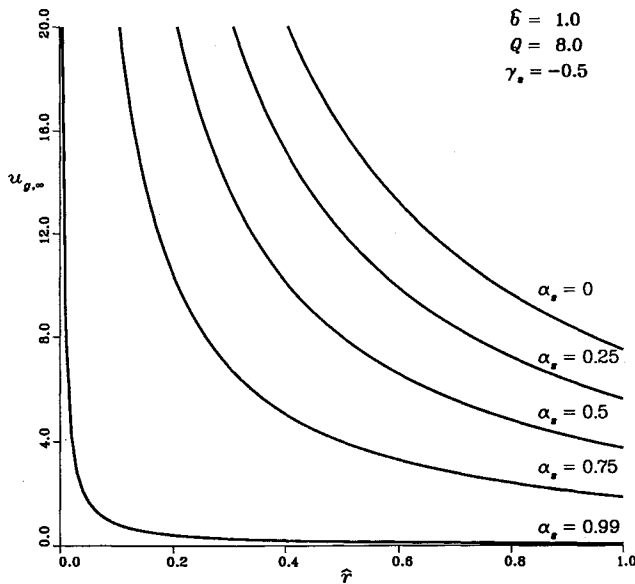


Fig. 3 Final gas velocity $u_{g,\infty}$ as a function of $\hat{\rho}$ for several values of α_s .

ature model (28–42), and so the burned temperature and final gas velocity are independent of the rate of interphase heat transfer.

The expressions (58) and (59) indicate that there are significant variations of the final burned temperature and gas velocity with pressure, since these quantities depend on the gas-to-solid density ratio $\hat{\rho}$, which in turn is proportional to \bar{p}_g^0 according to

$$\hat{\rho} \equiv \frac{\bar{p}_g^0}{\bar{p}_s} = \frac{\bar{W}_g \bar{p}_g^0}{\bar{p}_s \bar{R}^0 \bar{T}_u} = \frac{\bar{p}_g^0}{\bar{p}_s \bar{c}_s (1 - \gamma^{-1}) \bar{T}_u} \quad (60)$$

$$T(\xi) = \begin{cases} 1 + (T_m - 1) \exp \left[\frac{1 + \alpha_s (\hat{\rho} b - 1)}{1 + \alpha_s (\hat{l} - 1)} \xi \right], & \xi < 0 \\ B + (T_m - B) \exp \left[\frac{b(1 - \alpha_s) + \hat{\rho} b \alpha_s}{l(1 - \alpha_s) + \hat{l} \alpha_s} \xi \right], & 0 < \xi < \xi_r \\ T_b, & \xi > \xi_r \end{cases} \quad (65)$$

where γ is the ratio of specific heats for the gas. This important effect arises from the two-phase nature of the flow, coupled with the thermal expansion of the gas and the porosity of the solid, both of which strongly influence the degree of gas-phase convective transport of enthalpy relative to the reactive condensed phase. In the limit $\bar{p}_g^0 \rightarrow 0$ (i.e., $\hat{\rho} \rightarrow 0$), we see that $u_{g,\infty} \rightarrow \infty$ and $T_b \rightarrow T_b^0$, where

$$T_b^0 \equiv (1/\hat{b})(Q + 1 + \gamma_s) \quad (61)$$

Since there is effectively no gas-phase enthalpy content in this limit, T_b^0 is also the value of T_b in the limit of zero porosity ($\alpha_s \rightarrow 0$). Indeed, in dimensional terms, $\bar{T}_b^0 = (\bar{c}_s \bar{T}_u + \bar{Q} + \bar{\gamma}_s)/\bar{c}_g$, which is equivalent to that obtained in Ref. 5, where zero porosity of the condensed material was assumed and thermal expansion of the gas was neglected. For nonzero values of pressure and porosity, some of the heat released by the energetic material must be used to raise the temperature of the nonreacting product gas in the unburned solid from unity to T_b . Consequently, both T_b and the final gas velocity $u_{g,\infty}$ are decreasing functions of the nondimensional gas-phase density $\hat{\rho}$, which increases with pressure according to Eq. (60).

Plots of T_b and $u_{g,\infty}$ as a function of $\hat{\rho}$ for several values of α_s , are shown in Figs. 2 and 3, respectively.

In order to determine the burning-rate eigenvalue, we must complete our analysis of the liquid/gas region $\xi > 0$. In this regard, Eqs. (45) and (56) constitute two equations for T and α in this region, with u_g then determined by Eq. (53) and the eigenvalue Λ determined by the boundary conditions. In order to handle the Arrhenius nonlinearity, we exploit the largeness of the nondimensional activation energy N and analyze the problem in the asymptotic limit $N \gg 1$.

In the limit $N \rightarrow \infty$, all chemical activity is concentrated in a very thin region where T is within $\mathcal{O}(1/N)$ of T_b . Denoting the location of this thin zone by $\xi_r > 0$, we see that the semi-infinite liquid/gas region is comprised of a preheat zone ($0 < \xi < \xi_r$), where chemical activity is exponentially small, the thin reaction zone where the chemical reaction goes to completion, and a burned region $\xi > \xi_r$. Thus, we conclude from Eq. (45) that

$$\alpha = \begin{cases} \alpha_s, & \xi < \xi_r \\ 1, & \xi > \xi_r \end{cases} \quad (62)$$

and from Eq. (53)

$$u_g = \begin{cases} T - 1 \\ \hat{\rho}^{-1}(1 - \alpha_s + \alpha_s \hat{\rho})T_b - 1 = u_{g,\infty}, \end{cases} \quad \begin{matrix} \xi < \xi_r \\ \xi > \xi_r \end{matrix} \quad (63)$$

Since T is within $\mathcal{O}(1/N)$ of T_b in the reaction zone, the analysis of this thin region requires the use of a stretched coordinate (see below). As a result, T is continuous with respect to the $\mathcal{O}(1)$ outer variable ξ at $\xi = \xi_r$, and thus, the gas velocity jumps across $\xi = \xi_r$ by the amount

$$u_g|_{\xi=\xi_r^+} - u_g|_{\xi=\xi_r^-} = (1/\hat{\rho})(1 - \hat{\rho})(1 - \alpha_s)T_b \quad (64)$$

which is positive assuming the gas density is less than that of the unburned solid (i.e., $\hat{\rho} < 1$). Finally, using Eq. (62), Eq. (56) may be integrated a second time to completely determine the outer temperature profile

where

$$B \equiv \frac{(1 - \alpha_s)(1 + \gamma_s) + \hat{\rho} b \alpha_s}{b(1 - \alpha_s) + \hat{\rho} b \alpha_s} \quad (66)$$

and $T(\xi)$ for $\xi < 0$ was given by Eq. (57). The location ξ_r of the reaction zone, which appears as a sheet on the scale of the outer variable ξ , is thus determined by Eqs. (65) from continuity of T as

$$\xi_r = \frac{l(1 - \alpha_s) + \hat{l} \alpha_s}{b(1 - \alpha_s) + \hat{\rho} b \alpha_s} \ln \left(\frac{T_b - B}{T_m - B} \right) \quad (67)$$

The determination of the burning-rate eigenvalue Λ , as well as the spatial evolution of the variables α and u_g (which are discontinuous on the scale of the outer variable ξ), requires an analysis of the thin reaction-zone region in the vicinity of ξ_r . We thus introduce a stretched inner variable η and a normalized temperature variable Θ defined by

$$\Theta = \frac{T - 1}{T_b - 1}, \quad \eta = \beta(\xi - \xi_r) \quad (68)$$

where

$$\beta \equiv (1 - T_b^{-1})N \gg 1 \quad (69)$$

and seek solutions in the form of the expansions

$$\alpha \sim \alpha_0 + \beta^{-1}\alpha_1 + \beta^{-2}\alpha_2 + \dots \quad (70)$$

$$u_g \sim u_0 + \beta^{-1}u_1 + \beta^{-2}u_2 + \dots \quad (71)$$

$$\Theta \sim 1 + \beta^{-1}\theta_1 + \beta^{-2}\theta_2 + \dots \quad (72)$$

$$\theta_1(\alpha_0) = \begin{cases} \frac{\ell_\infty \left(\frac{\ell_\infty [l + (\hat{l} - l)\alpha_0] - \ell_\infty [l + (\hat{l} - l)\alpha_s]}{\ell_\infty \hat{l} - \ell_\infty [l + (\hat{l} - l)\alpha_s]} \right), & \hat{l} \neq l \\ \frac{\ell_\infty \left(\frac{\alpha_0 - \alpha_s}{1 - \alpha_s} \right), & \hat{l} = l \end{cases} \quad (83)$$

$$\Lambda \sim \beta(\Lambda_0 + \beta^{-1}\Lambda_1 + \beta^{-2}\Lambda_2 + \dots) \quad (73)$$

From Eq. (53), the coefficients in the expansion of u_g are given in terms of the α_i and θ_i according to

$$\begin{aligned} u_0 &= (\alpha_0 \hat{r})^{-1} [\alpha_0 + \alpha_s(\hat{r} - 1)]T_b - 1 \\ u_1 &= (\alpha_0 \hat{r})^{-1} \{ [\alpha_0 + \alpha_s(\hat{r} - 1)](T_b - 1)\theta_1 \\ &\quad + (\alpha_s/\alpha_0)(\hat{r} - 1)T_b\alpha_1 \} \end{aligned} \quad (74)$$

etc. Substituting these expansions into Eqs. (45) and (56), collecting coefficients of like powers of β , and requiring that the inner reaction-zone solution match with the outer solutions for $\xi < \xi_r$ and $\xi > \xi_r$ then leads to a sequence of problems for the recursive determination of the coefficients in Eqs. (70–73). In particular, at leading order the inner problem is given by

$$\frac{d\alpha_0}{d\eta} = r\Lambda_0(1 - \alpha_0)e^{\theta_1} \quad (75)$$

$$[l + (\hat{l} - l)\alpha_0] \frac{d\theta_1}{d\eta} = \frac{D}{T_b - 1} (1 - \alpha_0) \quad (76)$$

subject to the matching conditions

$$\alpha_0 \rightarrow \alpha_s, \quad \theta_1 \sim E\eta \quad \text{as } \eta \rightarrow -\infty \quad (77)$$

$$\alpha_0 \rightarrow 1, \quad \theta_1 \rightarrow 0 \quad \text{as } \eta \rightarrow +\infty \quad (78)$$

Here, D and E are defined as

$$D \equiv (b - \hat{b})T_b + Q, \quad E \equiv \frac{1}{T_b - 1} \frac{dT}{d\xi} \bigg|_{\xi=\xi_r^-} \quad (79)$$

where the latter is calculated from Eq. (65).

The problem (75–78) is readily solved by employing α_0 as the independent variable. Thus, using Eq. (75), Eq. (76) may be written as

$$r\Lambda_0[l + (\hat{l} - l)\alpha_0] e^{\theta_1} \frac{d\theta_1}{d\alpha_0} = \frac{D}{T_b - 1} \quad (80)$$

which is readily integrated from α_s (at $\eta = -\infty$) to any $\alpha_0 \leq 1$, to give

$$e^{\theta_1(\alpha_0)} = \frac{D}{(T_b - 1)r\Lambda_0} \int_{\alpha_s}^{\alpha_0} \frac{d\alpha_0}{l + (\hat{l} - l)\alpha_0} \quad (81)$$

Evaluating Eq. (81) at $\alpha_0 = 1$ (at which $\theta_1 = 0$), thus determines the leading-order coefficient Λ_0 in the expansion of the burning-rate eigenvalue as

$$\Lambda_0 = \begin{cases} \frac{D}{(T_b - 1)r(\hat{l} - l)} \left[\frac{\hat{l}}{l + (\hat{l} - l)\alpha_s} \right], & \hat{l} \neq l \\ \frac{D}{(T_b - 1)rl} (1 - \alpha_s), & \hat{l} = l \end{cases} \quad (82)$$

Substitution of this result in Eq. (80) for arbitrary α_0 then completely determines $\theta_1(\alpha_0)$ as

The determination of $\alpha_0(\eta)$, and hence, $\theta_1(\eta)$, then follows directly from Eq. (75). For example, when $\hat{l} = l$ (equal gas and liquid thermal conductivities), we obtain

$$\alpha_0(\eta) = \frac{\alpha_s + \exp[l^{-1}D(1 - \alpha_s)\eta/(T_b - 1)]}{1 + \exp[l^{-1}D(1 - \alpha_s)\eta/(T_b - 1)]} \quad (84)$$

where the matching condition (77) has been used to evaluate the constant of integration.

From Eq. (82) and the definition of Λ [see the last of Eqs. (27) and Eq. (73)], the leading-order expression for the dimensional propagation speed \bar{U} is given by

$$\bar{U}^2 \sim \frac{r(T_b - 1)\bar{A}e^{-N}}{\beta D \bar{\rho}_s \bar{c}_s} \bar{f}(\bar{\lambda}_g, \bar{\lambda}_l) \quad (85)$$

where the last factor, which contains the complete dependence of the burning rate on the thermal conductivities, is given by

$$\bar{f}(\bar{\lambda}_g, \bar{\lambda}_l) = \begin{cases} \frac{\bar{\lambda}_g - \bar{\lambda}_l}{\ell_\infty(\bar{\lambda}_g[\bar{\lambda}_l + (\bar{\lambda}_g - \bar{\lambda}_l)\alpha_s])}, & \bar{\lambda}_g \neq \bar{\lambda}_l \\ \bar{\lambda}_l/(1 - \alpha_s), & \bar{\lambda}_g = \bar{\lambda}_l \end{cases} \quad (86)$$

in which the second expression for the thermal conductivity factor \bar{f} is the formal limit of the first for the case of equal thermal conductivities of the liquid and gas phases. This factor collapses to that obtained in Ref. 5 in the limit $\alpha_s = 0$ (i.e., in the limit of zero porosity of the solid). It is readily shown that \bar{f} is an increasing function of both $\bar{\lambda}_g$ and $\bar{\lambda}_l$, individually (i.e., $\partial\bar{f}/\partial\bar{\lambda}_g > 0$ and $\partial\bar{f}/\partial\bar{\lambda}_l > 0$ for $\bar{\lambda}_g/\bar{\lambda}_l \neq 1$), so that the propagation speed increases as the thermal conductivity of either the liquid or the gas phase increases. In addition, the thermal conductivity of the phase having the higher thermal conductivity exerts the greater influence on \bar{U} , because a higher proportion of the heat is transferred through the more highly conducting phase. For example, in the limit $\bar{\lambda}_l/\bar{\lambda}_g \gg 1$, we have $\bar{f} \sim \bar{\lambda}_l/\ell_\infty[(1 - \alpha_s)\bar{\lambda}_l/\bar{\lambda}_g]$, whereas in the opposite regime $\bar{\lambda}_g/\bar{\lambda}_l \gg 1$, we have $\bar{f} \sim \bar{\lambda}_g/\ell_\infty(1/\alpha_s)$ for $0 < \alpha_s < 1$. Finally, we observe that to this leading order of approximation, \bar{U} does not depend on the thermal conductivity of the solid, and thus, the conductivities of the two phases that coexist in the reaction zone play the dominant role in determining the propagation speed. Plots of $\bar{f}/\bar{\lambda}_l$ vs $\bar{\lambda}_g/\bar{\lambda}_l$, for several values of α_s , are shown in Fig. 4.

Since \bar{U} is exponentially sensitive to the burned temperature through the largeness of the nondimensional activation energy $N = \bar{E}_l/\bar{R}^0\bar{T}_b = \bar{E}_l/\bar{R}^0\bar{T}_u\bar{T}_b$ in Eq. (85), the influence of pressure on the propagation speed is dominated by its effects on T_b (see Fig. 2). Thus, since increases in pressure serve to

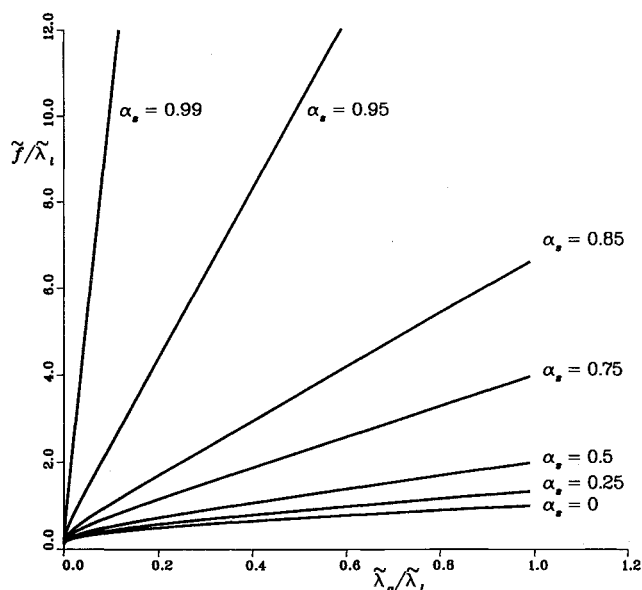


Fig. 4 Dependence of the propagation speed on the gas and liquid thermal conductivities. Shown is the thermal-conductivity factor $\tilde{\gamma}/\tilde{\lambda}_l$, normalized by $\tilde{\lambda}_l$, as a function of the gas-to-liquid thermal-conductivity ratio $\tilde{\lambda}_g/\tilde{\lambda}_l$ for several values of α_s .

decrease T_b in the present problem because of increases in the gas density as discussed above, the propagation speed is exponentially sensitive to changes in pressure.

The above conclusions regarding the propagation velocity were drawn for the case of equal gas- and condensed-phase temperatures (resulting from infinitely large values of the interphase heat transfer parameters K_{sg} and K_{lg}). In the next section it will be shown how small, but nonzero, temperature differences between coexisting phases affect these results by considering the effects of large, but finite, values of the interphase heat-transfer coefficients. It will be seen that this two-temperature regime can be treated as a perturbation of the single-temperature model and that the first effects of finite rates of interphase heat transfer are felt in the two-phase reaction zone.

V. Perturbation Analysis of the Two-Temperature Model

Returning to the two-temperature model (28–42), the first effects of finite rates of interphase heat transfer are felt as a perturbation of the single-temperature results when $K_{lg} \equiv \mathcal{O}(\beta^2)$, where β is the large activation-energy parameter defined in Eq. (69). Thus, we introduce scaled versions $k_{lg} \equiv k$ and k_{sg} of K_{lg} and K_{sg} , respectively, as

$$K_{lg} = \beta^2 k, \quad K_{sg} = \beta^2 k_{sg} \quad (87)$$

and seek solutions both outside and inside the reaction zone as expansions in appropriate powers of β^{-1} . In particular, the outer solutions are now expressed in the form

$$\begin{aligned} \alpha &\sim \alpha^{(0)} + \beta^{-2}\alpha^{(2)} + \dots \\ u_g &\sim u_g^{(0)} + \beta^{-2}u_g^{(2)} + \dots \\ T_{l,s,g} &\sim T^{(0)} + \beta^{-2}T_{l,s,g}^{(2)} + \dots \end{aligned} \quad (88)$$

where, again restricting consideration to the case $s = 0$, the leading-order terms are identical to the (outer) solution given in the previous section in the single-temperature limit $K_{lg}, K_{sg} \rightarrow \infty$, and perturbations from that solution enter at the same order as the order of K_{lg} and K_{sg} . That is, $\alpha^{(0)}$, $u_g^{(0)}$, and $T^{(0)}$ are given by Eqs. (62), (63), and (65), respectively, where,

as noted previously, the burned temperature T_b given by Eq. (58) is independent of interphase heat transfer effects.

To determine the burning-rate eigenvalue Λ , we again consider the inner reaction-zone problem. We thus introduce the inner variable η defined in Eq. (68), but now we must allow for temperature differences between the liquid and gas phases by defining (and expanding) two inner temperature variables Θ and Ψ as

$$\Theta = \frac{T_l - 1}{T_b - 1} \sim 1 + \beta^{-1}\theta_1 + \beta^{-2}\theta_2 + \dots \quad (89)$$

$$\Psi = \frac{T_g - 1}{T_b - 1} \sim 1 + \beta^{-1}\psi_1 + \beta^{-2}\psi_2 + \dots$$

Noting that the relationship (53) for u_g remains valid (provided T is reinterpreted as T_g in that equation), the remaining variables α and u_g , and the eigenvalue Λ , are then expanded as before [see Eqs. (70–74)]. The resulting leading-order inner problem obtained from substituting these expansions into Eqs. (30), (32), and (34) is given by

$$\frac{d\alpha_0}{d\eta} = r\Lambda_0(1 - \alpha_0)e^{\theta_1} \quad (90)$$

$$l(1 - \alpha_0)\frac{d\theta_1}{d\eta} + l\alpha_0\frac{d\psi_1}{d\eta} = \frac{D}{T_b - 1}(1 - \alpha_0) \quad (91)$$

$$l\frac{d}{d\eta}\left[(1 - \alpha_0)\frac{d\theta_1}{d\eta}\right] = -\frac{Q + bT_b}{T_b - 1}\frac{d\alpha_0}{d\eta} + rbk(\theta_1 - \psi_1) \quad (92)$$

subject to the matching conditions

$$\begin{aligned} \alpha_0 &\rightarrow \alpha_s, & \psi_1 &\rightarrow \theta_1 \sim E\eta \quad \text{as } \eta \rightarrow -\infty \\ \alpha_0 &\rightarrow 1, & \theta_1 &\rightarrow \psi_1 \rightarrow 0 \quad \text{as } \eta \rightarrow +\infty \end{aligned} \quad (93)$$

where D and E were defined in Eqs. (79) [with $T \equiv T^{(0)}$ in the latter, which is evaluated using Eq. (65)]. We observe that the effects of interphase heat transfer, while absent from the leading-order outer problem, are felt at leading order in the inner problem through Eq. (92).

The inner problem defined by Eqs. (90–93) is similar in form to that obtained in Ref. 5, and the same solution procedure is adopted here. In particular, having already restricted consideration to the physically realistic limit of high rates of interphase heat transfer according to Eqs. (87), we carry this argument one step further by considering the limit in which the scaled interphase parameter k itself is large. As a result, for $1 \ll k \ll \beta$, solutions to the leading-order inner problem can be sought as expansions in inverse powers of k as

$$\begin{aligned} \alpha_0 &\sim \chi + k^{-1}\chi_1 + k^{-2}\chi_2 + \dots \\ \theta_1 &\sim \theta + k^{-1}\tau_1 + k^{-2}\tau_2 + \dots \\ \psi_1 &\sim \theta + k^{-1}\phi_1 + k^{-2}\phi_2 + \dots \\ \Lambda_0 &\sim \mu + k^{-1}\mu_1 + k^{-2}\mu_2 + \dots \end{aligned} \quad (94)$$

where the fact that ψ_1 and θ_1 are the same to leading order follows from Eq. (92). Substitution of these expansions into Eqs. (90–93) then gives a sequence of problems for recursively determining the coefficients in Eqs. (94). The first two of these problems are given by

$$\frac{d\chi}{d\eta} = r\mu(1 - \chi)e^{\theta} \quad (95)$$

$$[l + (\hat{l} - l)\chi]\frac{d\theta}{d\eta} = q_1(1 - \chi) \quad (96)$$

$$l \frac{d}{d\eta} \left[(1 - \chi) \frac{d\theta}{d\eta} \right] = -q_2 \frac{d\chi}{d\eta} + rb(\tau_1 - \phi_1) \quad (97)$$

$$\chi \rightarrow \alpha_s, \quad \theta \sim E\eta, \quad \phi_1 \rightarrow \tau_1 \rightarrow 0 \quad \text{as } \eta \rightarrow -\infty \quad (98)$$

$$\chi \rightarrow 1, \quad \theta \rightarrow 0, \quad \tau_1 \rightarrow \phi_1 \rightarrow 0 \quad \text{as } \eta \rightarrow +\infty \quad (99)$$

$$\frac{d\chi_1}{d\eta} = r[\mu(1 - \chi)\tau_1 + \mu_1(1 - \chi) - \mu\chi_1]e^{\theta} \quad (100)$$

$$l(1 - \chi) \frac{d\tau_1}{d\eta} + \hat{l}\chi \frac{d\phi_1}{d\eta} = (l - \hat{l})\chi_1 \frac{d\theta}{d\eta} - q_1\chi_1 \quad (101)$$

$$l \frac{d}{d\eta} \left[(1 - \chi) \frac{d\tau_1}{d\eta} \right] = l \frac{d}{d\eta} \left(\chi_1 \frac{d\theta}{d\eta} \right) - q_2 \frac{d\chi_1}{d\eta} + rb(\tau_2 - \phi_2) \quad (102)$$

$$\chi_1 \rightarrow 0, \quad \phi_2 \rightarrow \tau_2 \rightarrow 0 \quad \text{as } \eta \rightarrow -\infty \quad (103)$$

$$\chi_1 \rightarrow 0, \quad \tau_2 \rightarrow \phi_2 \rightarrow 0 \quad \text{as } \eta \rightarrow +\infty \quad (104)$$

where

$$q_1 = \frac{D}{T_b - 1} = \frac{(b - \hat{b})T_b + Q}{T_b - 1}, \quad q_2 = \frac{Q + bT_b}{T_b - 1} \quad (105)$$

The subproblem defined by Eqs. (95) and (96), and the matching conditions on χ and θ , is identical to the leading-order problem (75–78) for the single-temperature model. Consequently, the solution for μ , the leading-order (with respect to k) approximation for Λ_0 , is given by Eq. (82). Similarly, the solution for $\theta(\chi)$, the leading-order approximation for both the liquid and gas-phase temperatures (θ_l and ψ_l), is given by Eq. (83), with the volume fraction α_0 replaced by its leading-order approximation χ . The scaled nondimensional excess $\tau_1 - \phi_1$ of the condensed-phase temperature over that of the gas phase is then determined from Eqs. (95) and (97) as

$$\tau_1 - \phi_1 = \frac{\mu}{b} (1 - \chi) e^{\theta(\chi)} \left\{ q_2 - q_1 \frac{l(1 - \chi)}{l + (\hat{l} - l)\chi} \times \left[2 + \frac{(\hat{l} - l)(1 - \chi)}{l + (\hat{l} - l)\chi} \right] \right\} \quad (106)$$

Since $q_2 > q_1$, Eq. (106) demonstrates that $\tau_1 - \phi_1$ is usually a positive quantity, especially for small gas-phase conductivities ($\hat{l} \ll l$), and/or as χ approaches unity. This is physically reasonable since, according to Eq. (7), the heat of reaction is initially deposited in the condensed phase, and there is now some resistance to heat transfer. However, in the event that the gas-phase conductivity were to exceed that of the liquid ($\hat{l}/l \gg 1$), then this temperature difference could become negative for smaller values of the volume fraction χ as a consequence of gas-phase heat conduction from the hotter, nearly burned portion to the less hot, mostly unburned part of the reaction zone.

To determine the effects of finite interphase heat transfer on the propagation speed, we need to calculate the correction μ_1 to the burning-rate eigenvalue, which requires a consideration of the next-order problem (100–104). Again transforming to χ as the independent coordinate according to Eq. (95), Eq. (100) may be solved for τ_1 , and the result may be employed in Eq. (106) to obtain an expression for ϕ_1 . Substitution of these results into Eq. (101) then produces a linear, second-order differential equation for $\chi_1(\chi)$, which when solved subject to the boundary conditions (98), (99), (103), and (104), determines μ_1 . For simplicity, we illustrate this development only for the case $\hat{l} = l$. Consequently, from Eqs. (82), (83), and (106), we have

$$\mu = (q_1/rb)^{-1}(1 - \alpha_s)$$

$$\theta = \mu[(\chi - \alpha_s)/(1 - \alpha_s)]$$

$$\phi_1 = \tau_1 - (q_1/rbl)^{-1}(\chi - \alpha_s)(1 - \chi)[q_2 - 2q_1(1 - \chi)] \quad (107)$$

where, from Eqs. (95) and (100), we obtain

$$\tau_1 = \frac{d\chi_1}{d\chi} + \frac{\chi_1}{1 - \chi} - \frac{\mu_1}{\mu} \quad (108)$$

Then, since Eqs. (95) and (101) and the above expressions for μ and θ imply that

$$(1 - \chi) \frac{d\tau_1}{d\chi} + \chi \frac{d\phi_1}{d\chi} + (1 - \alpha_s) \frac{\chi_1}{(\chi - \alpha_s)(1 - \chi)} = 0 \quad (109)$$

substituting the preceding expressions for τ_1 and ϕ_1 into Eq. (109) yields a second-order equation for χ_1 given by

$$\begin{aligned} \frac{d^2\chi_1}{d\chi^2} + \frac{1}{1 - \chi} \frac{d\chi_1}{d\chi} + \frac{(1 - \alpha_s)\chi_1}{(\chi - \alpha_s)(1 - \chi)^2} \\ = \frac{q_1 q_2}{rbl} \chi(1 + \alpha_s - 2\chi) - \frac{2q_1^2}{rbl} \chi(1 - \chi)(1 + 2\alpha_s - 3\chi) \end{aligned} \quad (110)$$

The general solution to Eq. (110) is expressible in closed form as

$$\begin{aligned} \chi_1 = (1 - \chi) \{ (\chi - \alpha_s)[c_1 + g(\chi)] \\ + c_2[(\chi - \alpha_s)^{-1/2}[(\chi - \alpha_s)/(1 - \chi)] - (1 - \alpha_s)] \} \end{aligned} \quad (111)$$

where c_1 and c_2 are constants of integration associated with the homogeneous solution of Eq. (110), and $g(\chi)$, which arises from the particular solution, is given by

$$\begin{aligned} g(\chi) = (q_1/rbl)^{-1} \{ (\alpha_s/2)[2(1 + 2\alpha_s)q_1 - (1 + \alpha_s)q_2]I_2(\chi) \\ + \frac{1}{3}[(1 + 3\alpha_s)q_2 - 2(1 + 6\alpha_s + 2\alpha_s^2)q_1]I_3(\chi) \\ + \frac{1}{3}[(4 + 5\alpha_s)q_1 - q_2]I_4(\chi) - \frac{6}{5}q_1I_5(\chi) \} \end{aligned} \quad (112)$$

where the indefinite integrals $I_n(\chi)$ are defined as

$$\begin{aligned} I_n(\chi) &= \int \frac{\chi^n}{(1 - \chi)(\chi - \alpha_s)^2} d\chi \\ &= \frac{1}{(1 - \alpha_s)^2} \left(\int \frac{\chi^n d\chi}{1 - \chi} + \int \frac{\chi^n d\chi}{\chi - \alpha_s} \right) + \frac{1}{1 - \alpha_s} \int \frac{\chi^n d\chi}{(\chi - \alpha_s)^2} \\ &= -\frac{\alpha_s^n}{1 - \alpha_s} (\chi - \alpha_s)^{-1} + \left(\frac{n\alpha_s^{n-1}}{1 - \alpha_s} + \frac{\alpha_s^n}{(1 - \alpha_s)^2} \right) \mu(\chi - \alpha_s) + \sum_{j=1}^{n-1} \frac{n!\alpha_s^{n-j-1}(\chi - \alpha_s)^j}{j(j+1)!(n-j-1)!(1 - \alpha_s)} \\ &\quad + \sum_{j=1}^n \frac{n!\alpha_s^{n-j}(\chi - \alpha_s)^j}{j \cdot j!(n-j)!(1 - \alpha_s)^2} - \frac{\mu(1 - \chi)}{(1 - \alpha_s)^2} + \sum_{j=1}^n \frac{n!(-1)^{j+1}(1 - \chi)^j}{j \cdot j!(n-j)!} \end{aligned} \quad (113)$$

for $n = 2, 3, 4$, and 5 . We now observe from Eqs. (111–113) that the solution for χ_1 automatically satisfies the boundary condition that $\chi_1 \rightarrow 0$ as $\chi \rightarrow 1$, whereas the condition that χ_1 vanish as $\chi \rightarrow \alpha_s$ determines c_2 as

$$c_2 = \frac{\alpha_s^3}{6(1 - \alpha_s)^2} \left[q_2 - 2 \left(1 - \frac{1}{10} \alpha_s^2 \right) q_1 \right] \quad (114)$$

We now may substitute Eq. (111) for χ_1 into the expression (108) for τ_1 , whereupon the requirement that τ_1 vanish as $\chi \rightarrow \alpha_s$ and as $\chi \rightarrow 1$ determines the remaining constant of integration c_1 and the scaled correction μ_1 to the burning-rate eigenvalue. In particular, as χ approaches unity, the latter is obtained directly as

$$\mu_1 = -\mu \frac{q_1(1 - \alpha_s)^2}{6rbl} \left[q_2 - \frac{1}{5} q_1(1 - \alpha_s)(4 + \alpha_s) \right] \quad (115)$$

which, since always $q_2 > q_1$, is less than zero for all α_s . Consequently, the propagation speed increases as the resistance to interphase heat transfer increases (i.e., as k decreases, since the magnitude of the correction to the eigenvalue Λ_0 to leading order is inversely proportional to k), consistent with the fact that this resistance causes the temperature of the liquid phase to exceed that of the gas, as discussed earlier. That is, the heat of reaction, which is deposited in the condensed phase, raises the temperature of this phase over what it would otherwise be if there were no resistance to interphase heat transfer, thereby increasing the (liquid) temperature-sensitive reaction rate.

VI. Summary

A multiphase flow theory has been developed for the deflagration of porous energetic materials, such as degraded nitramine propellants, that undergo exothermic reactions in a liquid layer to produce gaseous products. Both single- and two-temperature models were analyzed, the latter in a perturbative fashion for large, but finite, interphase heat-transfer coefficients. The combination of porosity and gas-phase thermal expansion was shown to lead to pressure-dependent temperatures, resulting in a significant pressure sensitivity for the burned temperature, and hence, the propagation speed. Formulas for the latter were derived for the case of steady, planar burning using the method of activation-energy asymptotics. It was demonstrated that increases in the conductivity of either phase in the liquid/gas reaction region lead to increases in the burning velocity, while increased resistance to interphase heat transfer generally has a similar effect by causing the condensed phase, where the heat of reaction is initially deposited, to have a higher temperature than that of the gas.

Acknowledgments

This work was supported by the U.S. Department of Energy under Contract DE-AC04-94AL85000 and by a Memorandum of Understanding between the Office of Munitions (Department of Defense) and the Department of Energy. The authors would like to thank R. Behrens, M. R. Baer, and A. C. Ratzel for fruitful discussions during the initiation phase of this research.

References

- ¹Drew, D. A., "Mathematical Modelling of Two-Phase Flow," *Annual Review of Fluid Mechanics*, Vol. 15, Annual Reviews Inc., Palo Alto, CA, 1983, pp. 261–291.
- ²Baer, M. R., and Nunziato, J. W., "A Two-Phase Mixture Theory for the Deflagration-to-Detonation Transition (DDT) in Reactive Granular Materials," *International Journal of Multiphase Flow*, Vol. 12, No. 6, 1986, pp. 861–889.
- ³Maksimov, E. I., and Merzhanov, A. G., "Theory of Combustion of Condensed Substances," *Combustion, Explosion, and Shock Waves*, Vol. 2, No. 1, 1966, pp. 25–31.
- ⁴Merzhanov, A. G., "The Theory of Stable Homogeneous Combustion of Condensed Substances," *Combustion and Flame*, Vol. 13, No. 2, 1969, pp. 143–156.
- ⁵Margolis, S. B., Williams, F. A., and Armstrong, R. C., "Influences of Two-Phase Flow in the Deflagration of Homogeneous Solids," *Combustion and Flame*, Vol. 67, No. 3, 1987, pp. 249–258.
- ⁶Margolis, S. B., and Williams, F. A., "Stability of Homogeneous-Solid Deflagration with Two-Phase Flow in the Reaction Zone," *Combustion and Flame*, Vol. 79, No. 2, 1990, pp. 199–213.
- ⁷Li, S. C., Williams, F. A., and Margolis, S. B., "Effects of Two-Phase Flow in a Model for Nitramine Deflagration," *Combustion and Flame*, Vol. 80, Nos. 3/4, 1990, pp. 329–349.
- ⁸Aldushin, A. P., "Heat Transfer and Convection Combustion Regimes of Porous Systems with Filtration of Heat Carrier," *Combustion, Explosion, and Shock Waves*, Vol. 26, No. 2, 1990, pp. 180–187.
- ⁹Shkadinsky, K. G., Shkadinskaya, G. V., Matkovsky, B. J., and Volpert, V. A., "Two-Front Traveling Waves in Filtration Combustion," *SIAM Journal on Applied Mathematics*, Vol. 53, No. 1, 1993, pp. 128–140.
- ¹⁰Aldushin, A. P., and Zeinenko, K. I., "Combustion of Pyrotechnic Mixtures with Heat Transfer from Gaseous Reaction Products," *Combustion, Explosion, and Shock Waves*, Vol. 27, No. 6, 1991, pp. 700–703.
- ¹¹Kuo, K. K., and Summerfield, M., "Theory of Steady-State Burning of Gas-Permeable Propellants," *AIAA Journal*, Vol. 12, No. 1, 1974, pp. 49–56.
- ¹²Ermolayev, B. S., Borisov, A. A., and Khasainov, B. A., "Comments on 'Theory of Steady-State Burning of Gas-Permeable Propellants,'" *AIAA Journal*, Vol. 13, No. 8, 1975, p. 1128.
- ¹³Gough, P. S., and Zwarts, F. J., "Modeling Heterogeneous Two-Phase Reacting Flow," *AIAA Journal*, Vol. 17, 1979, pp. 17–25.
- ¹⁴Gokhale, S. S., and Krier, H., "Modeling of Unsteady Two-Phase Reactive Flow in Porous Beds of Propellant," *Progress in Energy and Combustion Science*, Vol. 8, No. 1, 1982, pp. 1–39.